

Drift, creep and pinning of a particle in a correlated random potential

Heinz Horner

Institut für Theoretische Physik, Universität Heidelberg, Philosophenweg 19, D-69120 Heidelberg

To be published in Z.Physik B. Submitted Aug. 1995. Revised Oct. 5. 1995.

Abstract. The motion of a particle in a correlated random potential under the influence of a driving force is investigated in mean field theory. The correlations of the disorder are characterized by a short distance cutoff and a power law decay with exponent γ at large distances. Depending on temperature and γ , drift with finite mobility, creep or pinning is found. This is in qualitative agreement with results in one dimension. This model is of interest not only in view of the motion of particles or manifolds in random media, it also improves the understanding of glassy non-equilibrium dynamics in mean field models. The results, obtained by numerical integration and analytic investigations of the various scaling regimes in this problem, are compared with previous proposals regarding the long time properties of such systems and with replica calculations.

1 Introduction

This paper deals with the motion of a particle in a correlated random potential under the influence of a driving force. The correlations of the disorder are characterized by a short distance cutoff and a power law decay at larger distances with exponent γ . This problem has been solved in one dimension [1, 2, 3] and, depending on γ , drift with finite mobility, creep or pinning was found. Creep means that the particle moves with a mean velocity less than proportional to the driving force and in case of pinning the mean velocity is zero, unless the force exceeds some critical value.

In N dimensions a mean field treatment becomes exact for $N \rightarrow \infty$ and there is a close formal similarity to spin glass problems with long range interactions. The situation without external driving force has been treated within replica theory [4, 5] and also using a stochastic dynamics approach [6, 7]. Actually the more general case of the motion of a D -dimensional manifold in an $N \rightarrow \infty$ dimensional space was investigated. For finite N the mean field treatment is only an approximation. Nevertheless it might give some clue about a great variety of systems with disorder, for instance flux lines in superconductors or interfaces in random field systems.

The close formal relation to spin glass problems raises another set of questions. There has been a continuous interest in the dynamics of spin glasses and related systems. The pioneering work of Sompolinsky and Zippelius [8, 9] concentrated in part on an understanding of the replica theory and the hierarchical replica symmetry breaking scheme proposed by Parisi [10]. The basic assumption was about the existence of a hierarchy of diverging time scales with ultrametric properties. This point has been investigated further [11] introducing a long time scale \bar{t} associated with slow changes of the random interactions in this model. It could be shown that the above assumption meant that the long time contributions to the correlation and response functions have to be smooth functions of $x(t) = 1 - \ln t / \ln \bar{t}$ with $\bar{t} \rightarrow \infty$. It was later shown [12] that this led to inconsistencies which could not be resolved at that time.

There exists a variety of models with disorder where a replica treatment requires only single step replica symmetry breaking instead of the hierarchical scheme mentioned above. The resulting phase transition can be considered as discontinuous in contrast to the continuous transition observed in the SK-model and other cases requiring hierarchical replica symmetry breaking. A treatment via dynamics [6, 13, 14, 15] revealed a dynamic freezing temperature above the transition temperature obtained in replica theory. This is in contrast to the continuous transitions where the same transition temperature is found. Furthermore it could be shown [15] that the states which contribute to dynamics have a higher energy than the states relevant for the replica calculation. Numerical simulations of a learning process in a perceptron with binary bonds [14], another system with discontinuous transition, indicated that the replica result applies if the limit $\bar{t} \rightarrow \infty$ is performed first and then the limit $N \rightarrow \infty$, whereas the results obtained via dynamics hold for the opposite order. This observation suggests that in the thermodynamic limit the particular states most relevant for the replica calculation cannot be reached within any finite time. This picture is consistent with the fact that finding the best groundstate in a spin glass or perfect learning in a perceptron with binary bonds is a combinatorial hard problem which can-

not be solved in polynomial time. The replica treatment, on the other hand, is purely static and does not refer to any kind of dynamics. For a given physical situation the appropriate order of limits has of course to be found, keeping in mind that the longest equilibration times are likely to diverge exponentially with some power of N [16].

This raises the question whether similar discrepancies also show up in systems with continuous transition. The problem of the motion of a particle in a random potential under the influence of a driving force is in several aspects an appropriate model system to address this question. Prescribing the drift velocity v and calculating the force necessary to drive the particle, a long external time scale is defined by $\bar{t} \sim v^{-1}$. For times exceeding \bar{t} the system is supposed to reach a stationary non-equilibrium state, a so-called flow state, where correlation and response functions depend on differences of time only. This is of great advantage regarding numerical as well as analytic work. Depending on the exponent γ and on temperature, a continuous as well as a discontinuous transition can be found and therefore both cases can be studied on a single model.

The results presented in the following are based on numerical integrations of the dynamic mean field equations of this model, extending over more than thirty orders of magnitude in time and velocity. Such a wide range is actually necessary in order to understand the different scaling and crossover regimes emerging in this problem. Such a wide range of time scales is not unrealistic keeping in mind that phenomena might be observed on a scale of days or more with an intrinsic time scale of 10^{-12} to 10^{-16} seconds typical for vibrational or electronic degrees of freedom.

The numerical results are supplemented by exhaustive analytic work characterizing the different scaling regimes and focusing on their asymptotic properties and associated exponents. The characteristic time scales are obtained by matching between adjacent scaling regimes and are again governed by characteristic exponents.

The key result of the present investigation is the observation that the dynamics with a long but finite external time scale \bar{t} is ruled by three regimes:

- i) The FDT-regime describing local equilibrium at short times.
- ii) The intermediate plateau regime for times $t \sim \bar{t}^\xi$ with $0 < \xi < 1$.
- iii) The asymptotic regime for $t \sim \bar{t}$.

These regimes have additional substructures and associated additional internal time scales.

The plateau regime is the crucial link between short times and long times of the order of the external time scale. Its properties determine for instance whether

creep or pinning is found or whether the longest internal time scale is proportional to \bar{t} or $\bar{t}^{1+\eta}$ with $\eta > 0$. This question is of relevance for instance in the context of aging phenomena [17, 18, 19].

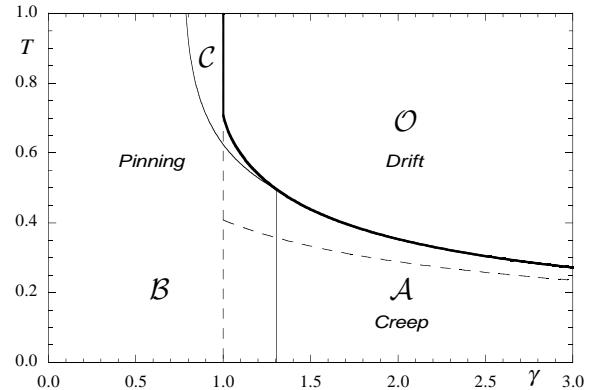


Figure 1: Phase diagram. \mathcal{O} : Drift phase with $v \sim F$ (driving force F , resulting velocity v). \mathcal{A} : Creep phase with $v \sim F^{1/\eta}$. \mathcal{B} and \mathcal{C} : Pinning phases with $v = 0$ for $F < F_p$. The phase diagram resulting from replica theory is also shown (dotted lines)

Depending on γ and temperature, different phases are found. The phase diagram resulting from the present investigations is shown in Fig.1. There is a phase with finite mobility (\mathcal{O}), another one with creep behavior (\mathcal{A}) and two more where pinning is observed (\mathcal{B} and \mathcal{C}). This is in qualitative agreement with the findings for the one-dimensional model [2], which indicates that the transitions are not an artifact of the mean field treatment. In all phases, except the high temperature phase \mathcal{O} , additional intermediate time scales exist, which diverge for $v \rightarrow 0$. There is, however, no ultrametric organization of time scales. This is in contrast to the common proposal [7, 9, 11, 15]. Moreover, the phase diagram suggested by replica theory [4, 5] or dynamics within the hypothesis of ultrametric time scales [6, 7] differs from the one obtained in the present investigation. For instance, $\gamma = 1$ has been predicted for the \mathcal{A} - \mathcal{B} phase boundary in contrast to $\gamma = 1.3044$ found at present. This leads to the conclusion that the states dominating the replica theory with broken symmetry are again not the same as those relevant for dynamics on long but finite time scales.

As a consequence of the assumption of ultrametricity in the organization of diverging time scales, the resulting correlation and response functions were not unique [9, 11]. The present investigation yields on the other hand unique results and this problem is therefore removed. The inconsistencies [12] mentioned above are also resolved in the sense that the proposed reparametrization of time $x(t) = 1 - \ln t / \ln \bar{t}$ is not appropriate.

There has recently been a growing interest in

the dynamics of glassy systems evolving from a non-equilibrium initial state [20, 21, 22, 23, 24, 25, 26]. The situation there is more complicated because the problem is no longer homogeneous in time and response and correlation functions depend on two time arguments t and t' . If, however, $t - t' \ll t'$, one expects a behavior similar to the one investigated at present with t' taking over the role of \bar{t} . Especially if both $t - t'$ and t' diverge with $(t - t')/t' \rightarrow 0$, one should also expect the appearance of intermediate time scales and associated scaling regimes. This possibility has not been considered at full depth in the above work.

For short time $t - t'$ correlation and response functions are related by fluctuation-dissipation theorems (FDT). This is also the case in the present investigation. The different phases have, however, different scenarios of how FDT's are violated at longer time scales. Since this happens for times $1 \ll t \ll \bar{t}$, similar phases are expected for the above mentioned relaxation processes. In this context the non-equilibrium dynamics of the spherical SK-model investigated recently by Cugliandolo and Dean [25] is of great interest, because this model does not require replica symmetry breaking in its low temperature phase.

The present paper is organized as follows: Section 2 contains the definition of the model and the dynamic mean field equations, which have the form of coupled nonlinear integro-differential equations. It also contains the definition of effective time dependent exponents, which are widely used in the following. Section 3 is devoted to the numerical integration of the dynamic mean field equations, to the presentation of results and to a preliminary identification of different time scales and scaling regimes. Section 4 contains analytic results and estimates regarding time scales and scaling properties. It starts with the FDT-solution valid for short time and continues with a discussion of various convolution type integrals entering the self-energies. In bypassing the QFDT-solution [6] and the hierarchical solution [7] are brought up. It is then shown how to evaluate the above integrals using the time dependent effective exponents. This leads to a reformulation of the original mean field equations in terms of a set of 15 coupled ordinary and first order differential equations. This appears complicated but it allows a discussion of different scaling regimes in which only closed subsets of these equations are relevant. These regimes are in the order of increasing time the FDT-regime, the plateau regime, where the correlation function $q(t)$ stays close to the asymptotic value q_c of the FDT-solution, and finally the asymptotic regime for times of the order of the external time scale v^{-1} . A concluding discussion follows in Section 5 and a brief derivation of the dynamic mean field equations is given in an appendix.

2 Formulation of the problem and dynamic mean field theory

2.1 The model

A particle is investigated which moves under the influence of an external force $\mathbf{F} = \{\sqrt{N}F, 0, \dots, 0\}$ in a random potential $V(\boldsymbol{\varrho})$. The coordinates of the particle are written as $\boldsymbol{\varrho} = \{\varrho_1 + \sqrt{N}vt, \varrho_2, \dots, \varrho_N\}$ assuming a mean velocity $\mathbf{v} = \{\sqrt{N}v, 0, \dots, 0\}$. This means that the components ϱ_i are measured in a frame moving with velocity $\sqrt{N}v$ along the 1-direction. The scaling with \sqrt{N} ensures a nontrivial limit $N \rightarrow \infty$. The system is at a temperature $T = \beta^{-1}$ and its Hamiltonian is

$$H = V(\boldsymbol{\varrho}) + \frac{1}{2}\mu_0\boldsymbol{\varrho}^2 - \mathbf{F}\cdot\boldsymbol{\varrho}, \quad (2.1)$$

where a confining potential $\frac{1}{2}\mu_0\boldsymbol{\varrho}^2$ might be added to the random potential and the potential of the driving force. The following investigation is, however, restricted primarily to $\mu_0 = 0$. The motion of the particle is governed by a Langevin equation

$$\partial_t \varrho_\alpha = -\beta \frac{\delta H}{\delta \varrho_\alpha} + \xi_\alpha \quad (2.2)$$

with Gaussian white noise

$$\langle \xi_\alpha(t) \xi_\beta(t') \rangle = 2 \delta_{\alpha\beta} \delta(t - t'). \quad (2.3)$$

The quenched disorder is also assumed to be Gaussian with

$$\begin{aligned} \overline{V(\boldsymbol{\varrho})} &= 0 \\ \overline{V(\boldsymbol{\varrho})V(\boldsymbol{\varrho}')} &= -N f\left(\frac{1}{N}(\boldsymbol{\varrho} - \boldsymbol{\varrho}')^2\right) \end{aligned} \quad (2.4)$$

and

$$f(x) = \frac{1}{2(1-\gamma)} (1+x)^{1-\gamma}. \quad (2.5)$$

The strength and the short range cutoff of the disorder as well as the diffusion constant are set to one. This model differs from the one studied earlier [4, 5, 6, 7] only by the addition of the driving force.

2.2 Dynamic mean field theory

The order parameters of the dynamic mean field theory are the correlation function

$$q(t - t') = \frac{1}{N} \sum_{\alpha} \overline{\langle [\varrho_\alpha(t) - \varrho_\alpha(t')]^2 \rangle} \quad (2.6)$$

and the response function

$$r(t - t') = \frac{T}{N} \sum_{\alpha} \overline{\delta \langle \varrho_\alpha(t) \rangle / \delta F_\alpha(t')}. \quad (2.7)$$

They obey the mean field equations [6, 7]

$$\partial_t r(t) = -\mu r(t) + \int_0^t ds w(s)r(s)r(t-s) \quad (2.8)$$

and

$$\begin{aligned} \partial_t q(t) = & 2 - \mu q(t) + \int_0^t ds w(s)r(s)q(t-s) \\ & - \int_0^\infty ds \left\{ 2[W(t+s) - W(s)]r(s) \right. \\ & \left. - [w(t+s)r(t+s) - w(s)r(s)]q(s) \right\} \end{aligned} \quad (2.9)$$

with

$$w(t) = -4\beta^2 f''(q(t) + v^2 t^2), \quad (2.10)$$

$$W(t) = 2\beta^2 f'(q(t) + v^2 t^2) \quad (2.11)$$

and

$$\mu = \mu_0 + \int_0^\infty ds w(s)r(s). \quad (2.12)$$

A brief derivation is given in the appendix. In the following $\mu_0 = 0$ is assumed.

In thermal equilibrium correlation and response functions are related by a fluctuation-dissipation theorem (FDT) which reads $\partial_t q(t) = 2r(t)$. This is violated in a non-equilibrium situation and

$$n(t) = \frac{1}{2r(t)} \partial_t q(t) - 1 \quad (2.13)$$

is introduced as measure of this FDT-violation.

Using this in (2.10) and (2.11)

$$\partial_t W(t) = -\left\{ [1 + n(t)]r(t) + v^2 t \right\} w(t) \quad (2.14)$$

is found. Combining (2.8), (2.9) and (2.13) one obtains

$$\begin{aligned} r(t)\partial_t n(t) = & - \int_0^t ds w(s)r(s)r(t-s) \\ & \times [n(t) - n(t-s)] \\ & + \int_0^\infty ds \left\{ w(t+s)r(t+s)r(s) \right. \\ & \times [n(t+s) - n(s)] \\ & \left. + v^2(t+s) w(t+s)r(s) \right\} \end{aligned} \quad (2.15)$$

and this equation can now be used instead of one of the original mean field equations (2.8) or (2.9).

Prescribing the drift velocity v the average of the force necessary to drive the particle is

$$\beta F = v \left\{ 1 + \int_0^\infty ds s w(s)r(s) \right\} \quad (2.16)$$

which is derived in the appendix.

2.3 Effective exponents

It is convenient to define

$$g(t) = tr(t) \quad (2.17)$$

and then (2.13) is written as

$$t\partial_t q(t) = 2\{1 + n(t)\}g(t). \quad (2.18)$$

In order to present the results of the numerical integration of the mean field equations effective time dependent exponents are introduced. They are also used in the evaluation of the convolution type integrals in the self-energies of the mean field equations (2.8) and (2.15). The first two exponents are

$$\nu(t) = t\partial_t \ln g(t) \quad (2.19)$$

and

$$\alpha(t) = -t\partial_t \ln w(t). \quad (2.20)$$

With

$$k(t) = t\partial_t n(t) \quad (2.21)$$

the third exponent

$$\kappa(t) = t\partial_t \ln k(t) \quad (2.22)$$

is defined.

3 Numerical results

3.1 Numerical procedure

The dynamic mean field equations to be solved consist of two integro-differential equations (2.8) and (2.15), a first order differential equation (2.13), the definition of $w(t)$, (2.10) and (2.5), and the integral (2.12) determining μ . The second integral in (2.15) and the integral (2.12) extend overall times and therefore, evaluating the solution at some t requires the knowledge of the solution at all times, not only at $s < t$. This means that the equations have to be iterated. This is the price one has to pay for investigating a steady state situation. A study of the relaxation from a non-equilibrium initial state on the other hand is free of this problem, but it requires to deal with functions depending on two time arguments.

The wide span of time arguments ranging from 10^{-4} to 10^{36} requires a nonuniform discretization. The present calculation uses a homogeneous discretization of $\ln t$. The convolution type integrals in (2.8) and (2.15) can be evaluated by numerical integration using the values stored at the points of the above grid for one of the functions of the integrand and an interpolation for the other function. Alternatively, an approximative evaluation of the integrals using effective exponents, described in Section 4.4 is possible. For the actual calculation both methods have been combined.

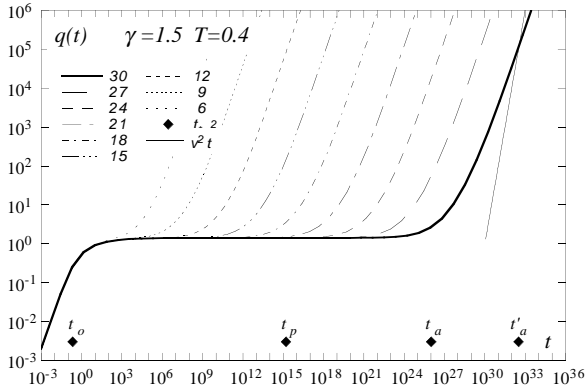


Figure 2: Correlation function $q(t)$ in phase \mathcal{A}

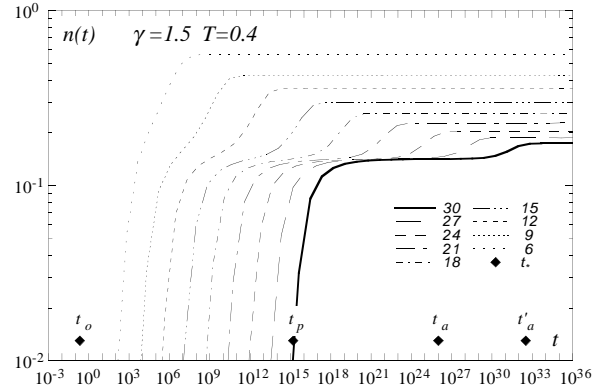


Figure 4: $n(t)$ in phase \mathcal{A}

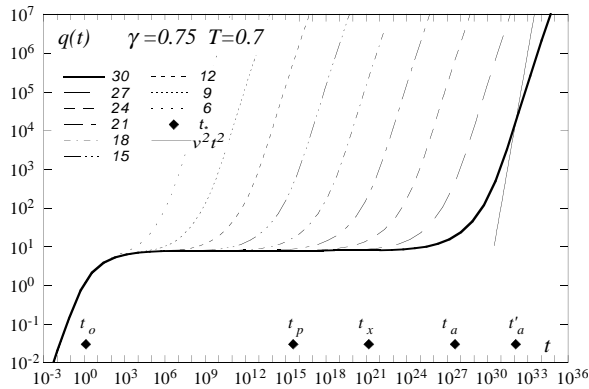


Figure 3: Correlation function $q(t)$ in phase \mathcal{B}

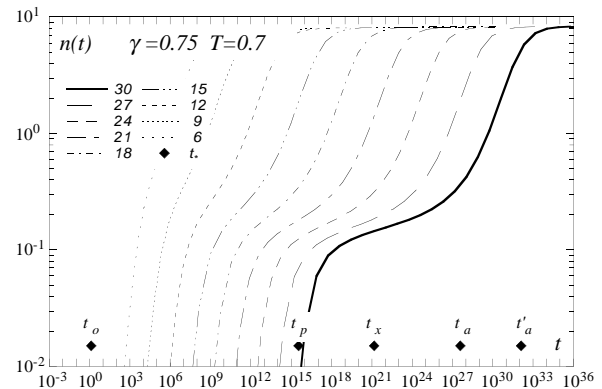


Figure 5: $n(t)$ in phase \mathcal{B}

The mean field equations in the form written in Section 4 consist of several coupled nonlinear differential equations of first order. They can be integrated forward or backward in time. In addition they have to be iterated. The situation resembles in some sense the problem of solving

$$\frac{dx(t)}{dt} = f(x(t)). \quad (3.1)$$

Integrating forward in t the solution typically approaches a fixed point $f(\bar{x}) = 0$ with $f'(\bar{x}) < 0$, whereas a fixed point with $f'(\bar{x}) > 0$ is reached integrating backward in t . Selecting an appropriate initial value $x(t_0)$ somewhere between a fixed point with $f'(\bar{x}) > 0$ and an adjacent one with $f'(\bar{x}) < 0$, the solution can easily be found by integration in both directions. For the complete set of equations such fixed point situations show up at the crossover between the various scaling regimes discussed below.

3.2 Results

The following figures show selected results obtained for $\{\gamma = 1.5; T = 0.4\}$ and $\{\gamma = 0.75; T = 0.7\}$, respectively. The first set of variables corresponds to a situ-

ation where the replica calculation [4, 5] requires single step replica symmetry breaking. This corresponds to a point in phase \mathcal{A} of the phase diagram, Fig.1. The second set corresponds to a point in phase \mathcal{B} and the corresponding replica treatment requires continuous replica symmetry breaking. The following figures show results obtained for various values of the drift velocity ranging from $v = 10^{-6}$ to $v = 10^{-30}$. In the following various velocity dependent characteristic time scales are introduced. Their values for $v = 10^{-30}$ are marked in the figures.

Figs.2 and 3 show the correlation function $q(t)$. The plateau value q_c is given by (4.3). In view of the argument $q(t) + v^2 t^2$ in (2.10) the value of $v^2 t^2$ for $v = 10^{-30}$ is also shown.

The function $n(t)$ defined in (2.13) is shown in Figs.4 and 5. It indicates the violation of the FDT, which holds for $t < t_p$. It develops a first plateau value for $t_p < t < t_a$ and a second one for $t > t'_a$. In phase \mathcal{A} this second value obviously depends on v . In phase \mathcal{B} the first plateau is not yet fully developed, even for $v = 10^{-30}$.

The time dependent effective exponents $\nu(t)$, (2.19), $\kappa(t)$, (2.22), and $\alpha(t)$, (2.20), are shown in Figs.6 to 11. Their properties are discussed below.

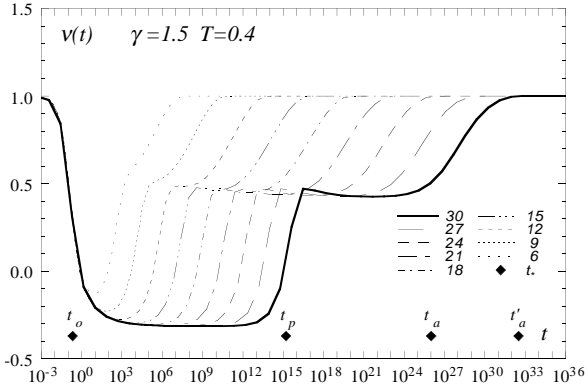


Figure 6: Effective exponent $\nu(t)$ in phase \mathcal{A}

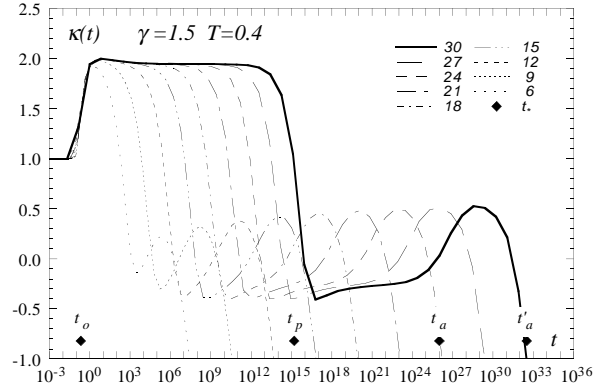


Figure 8: Effective exponent $\kappa(t)$ in phase \mathcal{A}

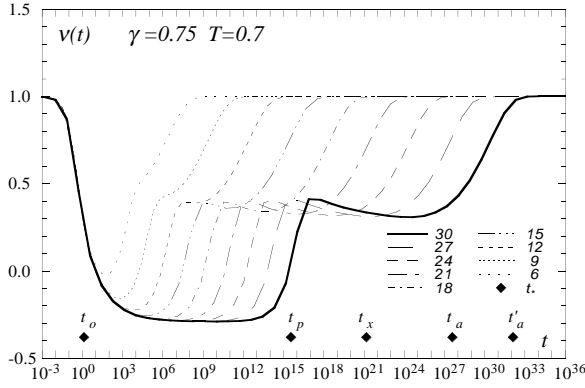


Figure 7: Effective exponent $\nu(t)$ in phase \mathcal{B}

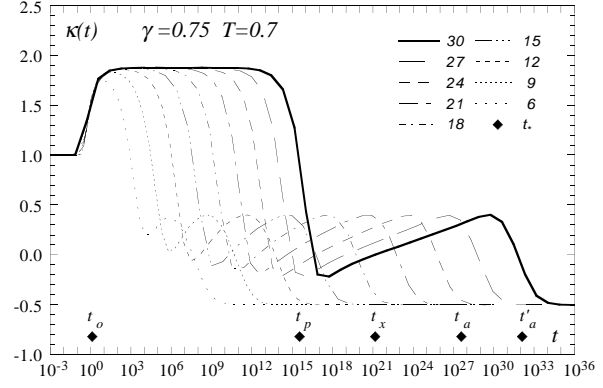


Figure 9: Effective exponent $\kappa(t)$ in phase \mathcal{B}

From the data several characteristic time scales can be extracted. They are shown in Figs.12 and 13 as functions of the velocity v . The time t_p is defined by $q(t_p) = q_c$ and it characterizes the center of the plateau. The next time scale t_x is relevant only for phase \mathcal{B} and it is given by $\kappa(t_x) = 0$. The time scale t_a is defined by $q(t_a) = 2q_c$ and t'_a by $q(t'_a) = 2v^2 t'_a$. A power law dependence is found for $v \rightarrow 0$.

3.3 Scaling regimes

The numerical results and analytic considerations described in Section 4 reveal the existence of various scaling regimes in the limit $v \rightarrow 0$.

3.3.1 FDT-regime

For finite $t \sim t_0$ one finds $n(t) \ll 1$ and fluctuation dissipation theorems hold. This can be understood as a situation where the particle stays within one valley of the energy landscape. The correlation function and $n(t)$ can be written as

$$q(t) = \hat{q}(t/t_0)$$

$$n(t) = \hat{b}(v) \hat{n}(t/t_0) \quad (3.2)$$

with $\hat{b}(v) \rightarrow 0$ for $v \rightarrow 0$. The time scale t_0 and the functions $\hat{q}(x)$ and $\hat{n}(x)$ do not depend on v . This regime is referred to as the FDT-regime.

3.3.2 Plateau-regime

With increasing t a plateau regime is found where $q(t) \approx q_c$. The corresponding time scale is $t_p = t_p(v)$ defined by $q(t_p) = q_c$ and the above functions obey the scaling form

$$\begin{aligned} q(t) &= q_c + \hat{a}(v) \hat{q}(t/t_p) \\ n(t) &= n_c + \hat{n}(t/t_p) \end{aligned} \quad (3.3)$$

which is consistent with $\nu(t) = \hat{\nu}(t/t_p)$ and $\kappa(t) = \hat{\kappa}(t/t_p)$.

The function $n(t)$, which is a measure of FDT-violation, reaches a plateau value n_c for $t \sim t_p$. In phase \mathcal{A} this plateau extends beyond the limits of the q -plateau.

In phase \mathcal{B} the plateau of $n(t)$ is not yet very pronounced, even at $v = 10^{-30}$, but it can be seen that the upper limits of the n -plateau and the q -plateau essentially coincide. The center of the n -plateau defines an

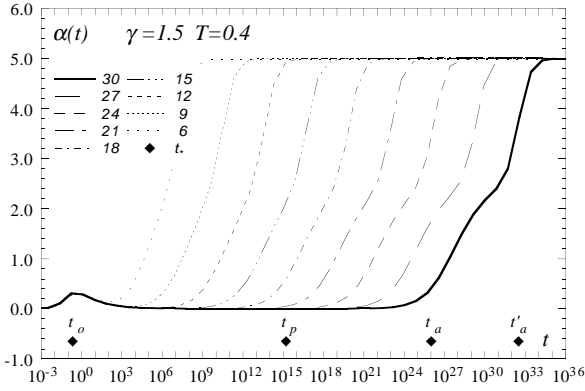


Figure 10: Effective exponent $\alpha(t)$ in phase \mathcal{A}

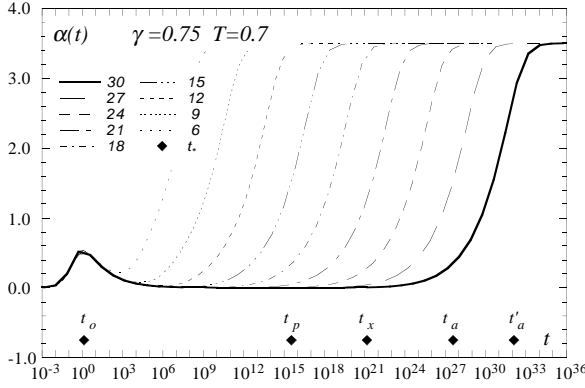


Figure 11: Effective exponent $\alpha(t)$ in phase \mathcal{B}

additional time scale $t_x = t_x(v)$ where $n(t_x) = n_c$ or $\kappa(t_x) = 0$. For $t \sim t_x$ a scaling form

$$n(t) = n_c + c(v)\hat{n}_x(c(v) \ln t/t_x) \quad (3.4)$$

will be derived.

In phase \mathcal{C} $n(t) \ll 1$ holds up to the upper end of the q -plateau and consequently the FDT-solution holds in the whole plateau regime.

3.3.3 Asymptotic regime

The lower end of the asymptotic regime is marked by a time scale $t_a = t_a(v)$ where $q(t_a) - q_c \sim q_c$. An appropriate choice is t_a such that $q(t_a) = 2q_c$. For $t \sim t_a$ a scaling form

$$\begin{aligned} q(t) &= \bar{q}(t/t_a) \\ n(t) &= n_c + \bar{b}(v)\bar{n}(t/t_a) \end{aligned} \quad (3.5)$$

with $\bar{b}(v) = 1$ in phase \mathcal{B} and \mathcal{C} is found.

Another time scale $t'_a = t'_a(v)$ can be defined such that $q(t'_a) = (v t'_a)^2$. In phase \mathcal{B} and \mathcal{C} both are proportional to v^{-1} , whereas $t_a(v) \sim v^{-1+\eta}$ and $t'_a(v) \sim v^{-1-\eta}$

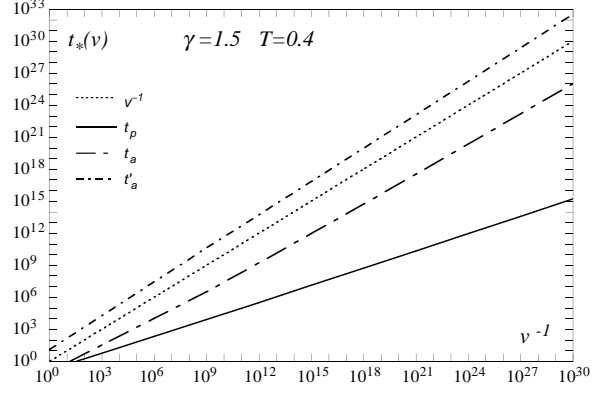


Figure 12: Characteristic time scales in phase \mathcal{A}

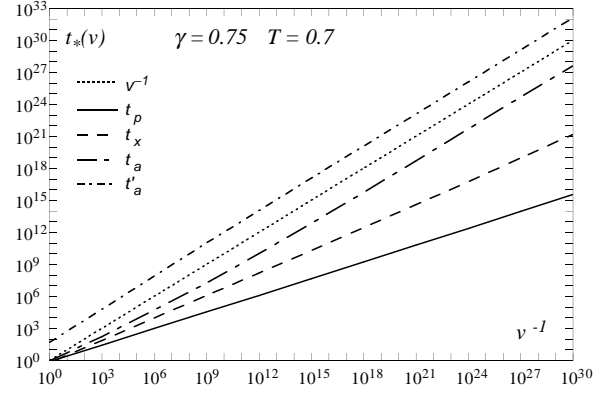


Figure 13: Characteristic time scales in phase \mathcal{B}

with $\eta > 0$ is found in phase \mathcal{A} . This requires for $t \sim t'_a$ the scaling form

$$n(t) = n_c + \bar{b}'(v) \bar{n}'(t/t'_a). \quad (3.6)$$

The existence of the exponent $\eta > 0$ is connected to the creep behavior observed in phase \mathcal{A} .

The above results now have to be verified by analytic investigations. This is done in the following sections.

4 Analytic results

4.1 FDT-solution

The shortest v -dependent time scale for $v \rightarrow 0$ is t_p with $1 \ll t_p \ll v^{-1}$. For $t \ll t_p$ one expects a solution which obeys the FDT and therefore $n(t) = 0$. This solution holds in phase \mathcal{O} for $v = 0$ and describes equilibrium within a single valley of the energy landscape in the other phases. The discussion of this solution follows standard arguments [6]. With (2.9), (2.14) and (2.18) one obtains

$$\begin{aligned} \partial_t q(t) &= 2 - \mu q(t) \\ &+ \int_0^t ds w(s)r(s)q(t-s), \end{aligned} \quad (4.1)$$

because the second integral in (2.9) vanishes. In order to demonstrate this, one realizes that its main contributions come from $s \sim t$ where $n(t) \approx 0$. With (2.17) and (2.18) $\partial_t q(t) \approx 2r(t)$ and with (2.14) $\partial_t W(t) \approx -w(t)r(t)$. This allows to write the integrand as a complete derivative with respect to s and to evaluate the integral resulting in 0, since $q(0) = 0$ and $W(t) \rightarrow 0$ for $t \rightarrow \infty$.

Eqs.(2.8) and (4.1) cannot be solved in closed form. It is, however, sufficient to investigate the solution for $t \rightarrow t_p$, where $q(t) \rightarrow q_c$, $\partial_t q(t) \rightarrow 0$ and $\partial_t r(t) \rightarrow 0$.

In leading order the integrals in both equations can be evaluated by taking into account only the contributions near the upper and lower bound, respectively. This yields from (2.8)

$$\mu = 2\beta^2 \{f'(0) - f'(q_c) - q_c f''(q_c)\} \quad (4.2)$$

and from (4.1)

$$f''(q_c)q_c^2 = -T^2. \quad (4.3)$$

The second equation is used to determine q_c . Elimination of μ in (4.2) using (2.12) yields with (2.10),(2.11) and (2.18)

$$\begin{aligned} q_c f''(q_c) &= -\frac{1}{2\beta^2} \int_{t_p}^{\infty} ds w(s) r(s) \\ &= \int_{t_p}^{\infty} ds \dot{q}(s) \frac{f''(q(s) + v^2 s^2)}{1 + n(s)}. \end{aligned} \quad (4.4)$$

This condition involving the solutions at long time scales will be used later.

In order to give estimates of the corrections to the leading order one assumes

$$tr(t) = g(t) \xrightarrow{t \rightarrow t_p} -\frac{1}{2}\nu_0 q_c (t/t_0)^{\nu_0} \quad (4.5)$$

with $\nu_0 < 0$. The time scale t_0 has yet to be determined. This leads to

$$\begin{aligned} q(t) &= q_c - 2 \int_t^{t_p} ds r(s) \\ &\xrightarrow{t \rightarrow t_p} q_c \left\{ 1 - (t/t_0)^{\nu_0} \right\}. \end{aligned} \quad (4.6)$$

This is now used in an analysis of the corrections in (2.8) where the leading order contains terms $\sim t^{\nu_0-1}$. The next to leading order $\sim t^{2\nu_0-1}$ results in

$$\begin{aligned} f''(q_c) \int_0^t ds \{r(s)r(t-s) - 2r(t)r(s)\} \\ = \{f''(q_c) + \frac{1}{2}f'''(q_c)q_c r(t)\} \{q_c - q(t)\}. \end{aligned} \quad (4.7)$$

With (4.5) the integral on the left hand side can be evaluated. Introducing

$$R_m = -\frac{q_c f'''(q_c)}{2f''(q_c)} \quad (4.8)$$

one obtains

$$\frac{\Gamma^2(1 + \nu_0)}{\Gamma(1 + 2\nu_0)} = R_m \quad (4.9)$$

which allows to determine the exponent ν_0 .

In order to get an estimate of the time scale t_0 one can use an interpolation formula

$$q(t) \approx q_c \left\{ 1 - (1 + t/t_0)^{\nu_0} \right\} \quad (4.10)$$

which gives the correct asymptotic behavior for $t \rightarrow t_p$. The requirement $q(t) \rightarrow 2t$ for $t \rightarrow 0$ yields

$$t_0 \approx -\frac{1}{2}\nu_0 q_c. \quad (4.11)$$

In the ergodic high temperature phase \mathcal{O} for $v = 0$ the FDT holds for all times and therefore with (2.12)

$$\mu = \frac{2f'(0)}{T^2}. \quad (4.12)$$

At the transition to one of the nonergodic phases the plateau develops and one finds with (4.2) and (4.3)

$$\begin{aligned} T_c^2 &= q_c f'(q_c), \\ f'(q_c) &= -q_c f''(q_c). \end{aligned} \quad (4.13)$$

A solution of these equations with finite T_c exists only for $\gamma > 1$. It is

$$\begin{aligned} q_c &= \frac{1}{\gamma - 1} \\ T_c &= \sqrt{\frac{1}{2}} \gamma^{-\gamma/2} (\gamma - 1)^{(\gamma-1)/2}. \end{aligned} \quad (4.14)$$

This is shown in Fig.1. The corresponding value obtained from replica theory [4, 5]

$$T_{c,1RSB} = \frac{1}{\sqrt{6\gamma}} \quad (4.15)$$

is always below the above value.

For $T > T_c$ in phase \mathcal{O} the FDT holds for all times and the force (2.16) is

$$\beta F = v \left\{ 1 + \int_0^{\infty} dt W(t) \right\}. \quad (4.16)$$

For $t \rightarrow \infty$ (2.8) yields $r(t) \rightarrow r_{\infty}$ and $q(t) \sim t$. Therefore the integral in (4.16) converges for $\gamma > 1$ and there exists a finite friction constant for $v \rightarrow 0$

4.2 Integrals and counterterms

For $t \gg 1$ the leading contributions to the integrals in (2.8) and (2.15) come from regions near the boundaries of integration. Subtracting those leads to residual integrals and a reformulation of the dynamic mean field equations. The following integrals are introduced:

$$\begin{aligned} J(t) &= \int_0^t ds \left\{ w(s)r(s)r(t-s) - w(t)r(t)r(t-s) \right. \\ &\quad \left. - w(s)r(s)r(t) + s w(s)r(s)\partial_t r(t) \right\}, \end{aligned} \quad (4.17)$$

$$\begin{aligned}
K(t) &= \int_0^\infty ds w(t+s)r(t+s)r(s) \\
&\quad \times \left\{ n(s) - n(s+t) \right\} \\
&\quad - \int_0^t ds w(t-s)r(t-s) \left\{ r(s)n(s) \right. \\
&\quad \left. - r(s)n(t) + (t-s)r(t)\partial_t n(t) \right\} \quad (4.18)
\end{aligned}$$

and

$$U(t) = v^2 \int_0^\infty ds (t+s)w(t+s)r(s). \quad (4.19)$$

Furthermore it is appropriate to define

$$D(t) = \int_t^\infty ds w(s)r(s) - w(t) \int_0^t ds r(s) \quad (4.20)$$

and

$$Z(t) = 1 + \int_0^t ds s w(s)r(s). \quad (4.21)$$

This allows to rewrite the mean field equation (2.8) in the form

$$Z(t) \partial_t r(t) = J(t) - D(t)r(t) \quad (4.22)$$

and (2.15) as

$$Z(t) r(t) \partial_t n(t) = U(t) - K(t). \quad (4.23)$$

4.3 QFDT- and hierarchical solution

With (4.20) and $n(t) \approx 0$ for $t < t_p$ the condition (4.4) means $D(t_p) = 0$.

Depending on γ for $v = 0$ a QFDT-solution and a hierarchical solution, respectively, have been proposed [6, 7]. These solutions can easily be obtained from the above equations. Especially the second scheme requires, however, assumptions which are not fulfilled. Nevertheless they are presented here for further reference.

4.3.1 QFDT-solution

In the QFDT-solution $n(t) = n_Q$ for $t > t_p$ is assumed. From (4.4) one finds

$$n_Q + 1 = -\frac{f'(q_c)}{q_c f''(q_c)}. \quad (4.24)$$

Without further analysis of the regime $t > t_p$ nothing can be said about the range of validity of this solution or about the force F . This solution was proposed to be valid for $\gamma > 1$ and it shows some similarity to the IRSB-calculation [4, 5].

4.3.2 Hierarchical solution

Assume that the integral in (2.8) for $t > t_p$ is completely determined by its contributions from the upper and lower bound, respectively. This means that $J(t) \approx 0$. As it turns out this is the essence of the proposal of the existence of an ultrametric organization of long time scales. Neglecting the derivative with respect to t in (4.22) results in $D(t) \approx 0$ for $t > t_p$.

Defining

$$m(q(t)) = \frac{1}{1+n(t)} \quad (4.25)$$

Eq.(4.20) yields

$$\int_q^\infty dq' f''(q') m(q') = f''(q) \int_0^q dq' m(q'). \quad (4.26)$$

This leads to the differential equation

$$\partial_q \ln m(q) = \frac{f''''(q)}{f'''(q)} - \frac{3f'''(q)}{2f''(q)} \quad (4.27)$$

which is solved for $q \geq q_c$ by

$$m(q) = m(q_c) \left\{ \frac{1+q}{1+q_c} \right\}^{-\frac{1}{2}(1-\gamma)} \quad (4.28)$$

using (2.5).

The integration constant $m(q_c)$ is obtained from (4.26) with $q = q_c$

$$m(q_c) = -\frac{f''''(q_c)q_c}{2f'''(q_c)} = R_m \quad (4.29)$$

with R_m given in (4.8). This is the solution obtained previously, assuming a hierarchical structure of long time scales [7].

4.4 Evaluation of integrals via effective exponents

The main problem in a discussion of the solutions of the mean field equations and also in their numerical integration is in the evaluation of the integrals listed in the previous section. In the following an approximative scheme is proposed, which turns out to be very accurate over the whole range of t . This scheme is based on the effective time dependent exponents, which have been introduced in Section 2.3. It allows to write and evaluate the integrals in the form

$$\int_0^1 dx x^{a-1} (1-x)^{b-1} = \frac{\Gamma(a)\Gamma(b)}{\Gamma(a+b)}. \quad (4.30)$$

As a first step in this program one introduces "dimensionless" quantities instead of the original ones given in (4.17) to (4.21):

$$\tilde{J}(t) = \frac{t J(t)}{w(t) g^2(t)}, \quad (4.31)$$

$$\tilde{K}(t) = \frac{t K(t)}{k(t) w(t) g^2(t)}, \quad (4.32)$$

$$\tilde{U}(t) = \frac{t U(t)}{k(t) w(t) g^2(t)}, \quad (4.33)$$

$$\tilde{D}(t) = \frac{D(t)}{w(t) g(t)}, \quad (4.34)$$

and

$$\tilde{Z}(t) = \frac{Z(t)}{t w(t) g(t)}. \quad (4.35)$$

The functions in the integrands are approximated by

$$s r(s) = g(s) \approx g(t) \left(\frac{s}{t}\right)^{\nu(t)}, \quad (4.36)$$

$$w(s) \approx w(t) \left(\frac{s}{t}\right)^{-\alpha(t)} \quad (4.37)$$

and

$$n(s) \approx n(t) + \frac{k(t)}{\kappa(t)} \left\{ \left(\frac{s}{t}\right)^{\kappa(t)} - 1 \right\}. \quad (4.38)$$

This ansatz fulfills (2.19), (2.20), (2.21) and (2.22) for $s = t$. The integrals $\tilde{J}(t)$ and $\tilde{K}(t)$ are now of the form proposed above (for the first integral in (4.18) a trivial substitution of variables is necessary) and can be evaluated using (4.30) provided $a > 0$ and $b > 0$. Otherwise counterterms are required cancelling the poles of the Γ -functions. The last three terms in (4.17) are of this kind. Depending on the values of the effective exponents further counterterms might be required.

This yields (in the following the arguments t are dropped)

$$\begin{aligned} \tilde{J} &\approx \frac{\Gamma(\nu - \alpha)\Gamma(\nu)}{\Gamma(2\nu - \alpha)} \\ &\quad - \frac{1}{\nu} - \frac{1}{\nu - \alpha} + \frac{\nu - 1}{\nu + 1 - \alpha} \end{aligned} \quad (4.39)$$

and

$$\begin{aligned} \tilde{K} &\approx \frac{1}{\kappa} \left\{ \frac{\Gamma(\nu + \kappa)\Gamma(1 + \alpha - 2\nu - \kappa)}{\Gamma(1 + \alpha - \nu)} \right. \\ &\quad - \frac{\Gamma(\nu)\Gamma(1 + \alpha - 2\nu - \kappa)}{\Gamma(1 + \alpha - \nu - \kappa)} \\ &\quad + \frac{\Gamma(\nu - \alpha)\Gamma(\nu)}{\Gamma(2\nu - \alpha)} - \frac{\Gamma(\nu - \alpha)\Gamma(\nu + \kappa)}{\Gamma(2\nu + \kappa - \alpha)} \\ &\quad \left. - \frac{\kappa}{\nu - \alpha + 1} \right\}. \end{aligned} \quad (4.40)$$

The integral (4.33) is given for $\nu > 0$ and $\alpha - \nu > 1$ by

$$\tilde{U} \approx \frac{v^2 t^2}{k g} \frac{\Gamma(\nu)\Gamma(\alpha - \nu - 1)}{\Gamma(\alpha - 1)} \quad (4.41)$$

otherwise it is approximated by

$$\tilde{U} \approx \frac{v^2 t Z(\infty)}{k w g^2}. \quad (4.42)$$

For $\alpha - \nu > 1$ (4.35) becomes

$$\tilde{Z} \approx \frac{Z(\infty)}{t w g} \quad (4.43)$$

otherwise

$$\tilde{Z} \approx \frac{1}{1 + \nu - \alpha}. \quad (4.44)$$

The mean field equations (4.22) and (4.23) are rewritten as

$$\{\nu - 1\} \tilde{Z} = \tilde{J} - \tilde{D} \quad (4.45)$$

and

$$\tilde{Z} = \tilde{U} - \tilde{K}. \quad (4.46)$$

The exponent α , (2.20), is

$$\alpha = -2g \{1 + n + u\} \frac{f'''(q + v^2 t^2)}{f''(q + v^2 t^2)} \quad (4.47)$$

with

$$u = \frac{v^2 t^2}{g}. \quad (4.48)$$

Differentiation of (4.20) yields with (4.34)

$$t \partial_t \tilde{D} = \{\alpha - \nu\} \tilde{D} - 2\{1 - [1 + n + u] R\} \quad (4.49)$$

with

$$R = - \frac{f'''(q + v^2 t^2)}{f''(q + v^2 t^2)} \int_0^t ds r(s). \quad (4.50)$$

The complete set of mean field equations now involves 15 functions of time: q , r , g , n , k , ν , κ , α , u , R , \tilde{D} , \tilde{J} , \tilde{K} , \tilde{U} and \tilde{Z} . The corresponding 15 equations are: (2.17), (2.18), (2.19), (2.21), (2.22), (4.39), (4.40), (4.41/4.42), (4.43/4.44), (4.45), (4.46), (4.48), (4.47), (4.49) and (4.50).

Some of the variables can easily be eliminated, but even then one is left with 5 differential equations of first order and 2 implicit ordinary equations for 7 of the above functions of time. This certainly looks complicated. On the other hand, in each of the scaling regimes to be discussed below only a subset of variables and equations has to be looked at.

4.5 The plateau regime

Having discussed the FDT-solution in Section 4.1 already, the investigation of the plateau regime follows next. This regime is characterized by $|q(t) - q_c| \ll q_c$. Further simplifications are due to $t^2 v^2 \ll q_c$. Consequently R defined in (4.50) can be replaced by the constant R_m given in (4.8). Furthermore $\tilde{U} \approx 0$ and $u \approx 0$ can be used. From (2.20) with (2.10) one finds $\alpha \approx 0$ and then (4.44) yields $\tilde{Z} \approx \frac{1}{1 + \nu}$.

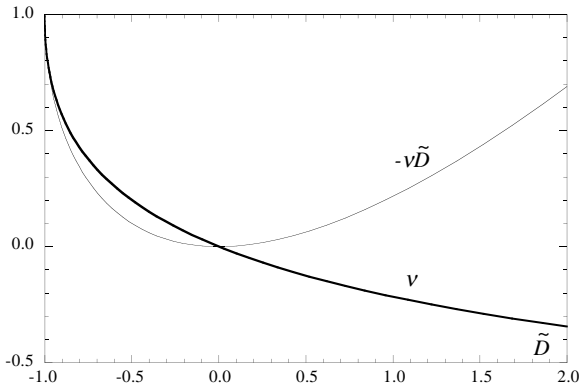


Figure 14: $\nu(\tilde{D})$ and $-\tilde{D}\nu(\tilde{D})$ as functions of \tilde{D} , see text.

Eqs.(4.39), (4.45) and (4.44) determine $\nu = \tilde{\nu}(\tilde{D})$ as a function of \tilde{D} , shown in Fig.14.

Eqs.(4.40) and (4.46) are solved by

$$\kappa(t) = 1 - 3\nu(t). \quad (4.51)$$

Eq. (4.49) now reads

$$t\partial_t \tilde{D}(t) = -\tilde{\nu}(\tilde{D}(t))\tilde{D}(t) - 2\{1 - [1 + n(t)]R_m\}. \quad (4.52)$$

The remaining set of equations to be solved consists of (2.21), (2.22), (4.39), (4.44), (4.45), (4.51) and (4.52). Time enters only via derivatives of the form $t\partial_t$ and therefore a family of scale invariant solutions exists. This means that the whole family can be written as a set of functions depending only on t/t_p with arbitrary t_p . This is in accordance with the scaling form proposed in (3.3).

The time scale $t_p \gg t_0$ can now be fixed such that $\tilde{D}(t_p) = 0$ and as a consequence $\nu(t_p) = 0$ and $\kappa(t_p) = 1$. Integrating (4.52) down to $t \ll t_p$ a stable fixpoint $\tilde{D}(t) \rightarrow \tilde{D}_0 > 0$ is reached with

$$-\tilde{\nu}(\tilde{D}_0)\tilde{D}_0 = 2\{1 - R_m\} \quad (4.53)$$

and $n(t) \rightarrow 0$. Eq.(4.9) yields $\nu(\tilde{D}_0) = \nu_0$.

For $t_0 \ll t \ll t_p$ the function $q(t)$ can be matched to the asymptotic FDT-solution (4.6) and

$$\hat{a}(v) = (t_p/t_0)^{\nu_0} \quad (4.54)$$

results for the scale factor in (3.3) where $t_p = t_p(v)$ has to be determined later by matching to the asymptotic regime. It can be shown that the above fixing of t_p is equivalent to the original definition $q(t_p) = q_c$ within a factor close to 1.

The discussion of the asymptotes for $t \gg t_p$, still within $|q(t) - q_c| \ll q_c$, is more involved. Neglecting the derivative with respect to time in (4.52) one gets

$$-\tilde{D}\tilde{\nu}(\tilde{D}) = 2\{1 - (1 + n)R_m\} \quad (4.55)$$

which now determines $\tilde{D} = \tilde{D}_1(n)$, $\nu_1 = \tilde{\nu}(\tilde{D}_1(n))$ and $\kappa_1 = \tilde{\kappa}(\tilde{D}_1(n)) = 1 - 3\tilde{\nu}(\tilde{D}_1(n))$.

There is a special value n_x such that $\tilde{\kappa}(\tilde{D}_1(n_x)) = 0$ with $\tilde{D}_1(n_x) = \tilde{D}_x \approx -0.700084$. This value is found from (4.52) as

$$n_x = \frac{1 + \frac{1}{6}\tilde{D}_x}{R_m} - 1. \quad (4.56)$$

Expanding

$$\tilde{\kappa}(\tilde{D}_1(n)) \approx (n - n_x)\kappa' \quad (4.57)$$

with $\kappa' > 0$, Eqs.(2.21) and (2.22) can be integrated in closed form. The real solutions are

$$n(t) = n_x - \frac{2c}{\kappa'} \coth(c \ln(t/t_x)) \quad (4.58)$$

and

$$n(t) = n_x + \frac{2c}{\kappa'} \tan(c \ln(t/t_x)) \quad (4.59)$$

with constants of integration c and t_x .

There are now two characteristic values for $n(t)$, the value n_Q defined in (4.24) and n_x defined above in (4.56). Both are functions of T and γ .

The relative magnitude of n_Q and n_x determines which of the above solutions has to be selected, as will be discussed in the following. This, on the other hand, determines ultimately whether creep or pinning is observed and therefore the different phases are characterized by their values of n_Q and n_x . Phase \mathcal{A} is defined as the region where $n_x > n_Q > 0$, phase \mathcal{B} has $n_Q > n_x > 0$ and $n_Q > 0 > n_x$ holds in phase \mathcal{C} . The ergodic phase \mathcal{O} with finite friction has already been discussed in Section 4.1

4.5.1 Phase \mathcal{A}

The numerical results shown in Fig.4 indicate a plateau of $n(t)$ extending to times beyond the upper boundary of the q -plateau. This suggests that the solution (4.58) has to be used for $t > t_p$. The choice $t_x \sim t_p$ yields the scaling form (3.3). For $t \gg t_p$ the requirement $n(t) \rightarrow n_Q < n_x$ determines

$$c = \frac{\kappa'}{2} (n_x - n_Q) \approx -\frac{\kappa_1}{2} \quad (4.60)$$

with $\kappa_1 = \tilde{\kappa}(\tilde{D}_1(n_Q))$. The parameter n_Q is later shown to agree with the value obtained for the QFDT-solution (4.24).

For $t \gg t_p$ the above equations yield with $\nu_1 = \tilde{\nu}(\tilde{D}_1(n_Q)) > 0$ and $\kappa_1 = 1 - 3\nu_1 < 0$

$$\begin{aligned} q(t) &\rightarrow q_c + (t_p/t_0)^{\nu_0} (t/t_p)^{\nu_1} \hat{q}_1 \\ n(t) &\rightarrow n_Q - (t/t_p)^{\kappa_1} \hat{n}_1. \end{aligned} \quad (4.61)$$

For $v \rightarrow 0$ the constants \hat{q}_1 and \hat{n}_1 depend only on γ and T .

For $t \ll t_p$

$$n(t) \rightarrow \hat{n}_0 (t/t_p)^{\kappa_0} \quad (4.62)$$

with constant \hat{n}_0 and $\kappa_0 > 0$. Matching at $t_0 \ll t \ll t_p$ yields the scale factor

$$\dot{b}(v) = (t_0/t_p)^{\kappa_0} \quad (4.63)$$

in (3.2). The time scale $t_p = t_p(v)$ is still open and has to be determined later by matching to the asymptotic regime. The same holds for n_Q .

4.5.2 Phase \mathcal{B}

The plateau of $n(t)$ in this phase extends only to the upper boundary of the q -plateau, as shown in Fig.5. This indicates that solution (4.59) now has to be used for $t > t_p$. Its range of validity is restricted to $-\frac{1}{2}\pi < c \ln(t/t_x) < \frac{1}{2}\pi$ or $e^{-\pi/2c} t_x < t < e^{\pi/2c} t_x$. Later it is shown that this range increases for $v \rightarrow 0$ and therefore $c = c(v) \rightarrow 0$ for $v \rightarrow 0$. For $t \rightarrow t_p$ the solution should not depend on c , which is the case for the choice

$$t_x = e^{\pi/2c} t_p. \quad (4.64)$$

For $t_p \ll t \ll e^{\pi/c} t_p$ the second term in (4.59) is a small correction and the proposed scaling form (3.3) and (3.4) holds over the whole range $t_0 \ll t \ll e^{\pi/c} t_p$.

With $\kappa_1 = \tilde{\kappa}(\tilde{D}_1(n_x)) = 0$ and $\nu_1 = \tilde{\nu}(\tilde{D}_1(n_x)) = \frac{1}{3}$, $q(t)$ has again the asymptotic form (4.61) for $t \gg t_p$ and the scale factor $\dot{b}(v)$ is given by (4.63). In this phase the quantities to be determined later by matching to the asymptotic regime are $t_p = t_p(v)$ and $t_x = t_x(v)$.

4.5.3 Phase \mathcal{C}

In this phase with $n_x < 0$ again solution (4.58) has to be used. Since now $\kappa_1 = \tilde{\kappa}(\tilde{D}_1(n_x)) > 0$ and $n(t_p) \ll 1$, the appropriate choice of the parameters is

$$\frac{2c}{\kappa'} = -n_x; \quad c = \frac{1}{2}\kappa_1. \quad (4.65)$$

This yields for $t_x \gg t_p$ and $t_p \ll t \ll t_x$

$$n(t) \approx -2n_x (t/t_x)^{\kappa_1} \ll 1 \quad (4.66)$$

which means that (3.3) is fulfilled with $n(t) \approx 0$.

The asymptotic form of $q(t)$ is again (4.61) with $\nu_1 = \tilde{\nu}(\tilde{D}_1(0))$. Again the quantities to be determined later by matching to the asymptotic regime are $t_p = t_p(v)$ and $t_x = t_x(v)$.

4.6 The asymptotic regime

The discussion so far did not depend on the actual choice of the drift velocity v . On the other hand, there are parameters not determined yet. These are the time scale $t_p(v)$ for all phases and the second time scale $t_x(v)$ for

phase \mathcal{B} and \mathcal{C} . For phase \mathcal{A} it has to be shown that n_Q actually agrees with the value obtained in the QFDT-solution, (4.24).

The velocity v enters the full set of mean field equations in $\tilde{U}(t)$, (4.41/4.42), at various places in the argument of $f(q(t) + v^2 t^2)$ and its derivatives, and in the definition of $u(t)$, (4.48). In order to obtain the scaling form proposed in (3.5) for $t \sim t_a$ it is necessary that $\tilde{U}(t)$ can be written as $\tilde{U}(t) = \bar{U}(t/t_a)$, which is the case for

$$\frac{v^2 t_a^2(v)}{\bar{b}(v)} = 1 \quad (4.67)$$

assuming the proposed scaling form in (4.41/4.42).

For $t \ll t_a$ the solution in the asymptotic regime has to match the solution valid in the plateau regime obtained in the preceding section for $t \gg t_p$. This means

$$q(t) \xrightarrow[t \rightarrow t_p]{} q_c + (t/t_a)^{\nu_1} \bar{q}_0 \quad (4.68)$$

with constant \bar{q}_0 . Comparison with (4.61) yields

$$(t_p/t_0)^{\nu_0} t_p^{-\nu_1} \sim t_a^{-\nu_1}; \quad t_p \sim t_0^{1-\zeta} t_a^\zeta \quad (4.69)$$

with

$$\zeta = \frac{\nu_1}{\nu_1 - \nu_0}. \quad (4.70)$$

The discussion of $n(t)$ has to be done for the different phases separately.

4.6.1 Phase \mathcal{A}

Following (3.5) one can write

$$n(t) \rightarrow n_Q - (t/t_a)^{\kappa_1} \bar{b} \bar{n}_0 \quad (4.71)$$

with constant \bar{n}_0 and $\bar{b} = \bar{b}(v)$. Comparison with (4.61) results in

$$\bar{b} \sim (t_a/t_p)^{\kappa_1}. \quad (4.72)$$

Using this in (4.67) one finds with (4.69)

$$\begin{aligned} t_a &\sim v^{-1+\eta} t_0^\eta \\ t_p &\sim v^{-(1-\eta)\zeta} t_0^{1-(1-\eta)\zeta} \end{aligned} \quad (4.73)$$

with

$$\eta = \frac{\nu_0 \kappa_1}{2(\nu_1 - \nu_0) + \nu_0 \kappa_1}. \quad (4.74)$$

Since $\nu_1 > 0$, $\nu_0 < 0$ and $\kappa_1 < 0$ one finds $\eta > 0$.

For $t \sim t_a$ the remaining v -dependence in the mean field equations is not of relevance, since

$$v^2 t^2 = (v t_0)^{2\eta} (t/t_a)^2 \ll \bar{q}(t/t_a) \quad (4.75)$$

and

$$u(t) = (v t_0)^{2\eta} (t/t_a)^2 / \bar{g}(t/t_a) \ll 1 \quad (4.76)$$

with $u(t)$ defined in (4.48) and $\bar{g}(t/t_a) = g(t)$.

For $t \gg t_a$ one obtains $\nu(t) \rightarrow 1$, $r(t) \rightarrow \bar{r}_1/t_a$ and $q(t) \rightarrow \bar{q}_1 t/t_a$ where \bar{r}_1 and \bar{q}_1 are constants. This follows immediately from (4.43) and (4.45) realizing that $\tilde{Z}(t)$ diverges $\sim t^{\alpha-2}$, whereas the right hand side of (4.45) remains finite for $t \gg t_a$. This defines an even longer time scale

$$t'_a \sim v^{-1-\eta} t_0^{-\eta} \quad (4.77)$$

where $q(t'_a) = (vt'_a)^2$.

For $t_a \ll t \ll t'_a$ Eq. (2.20) yields $\alpha \rightarrow \gamma + 1$. Investigating Eq.(4.46) one observes that $\tilde{Z}(t)$, (4.43), diverges $\sim t^{\alpha-2}$ and $\tilde{U}(t)$, (4.41), $\sim t^{1-\kappa}$, whereas $\tilde{K}(t)$, (4.40) remains finite. This means $\kappa(t) \approx 3 - \alpha(t)$ and $\kappa(t) \rightarrow \kappa_2 = 2 - \gamma$. For $\gamma < 2$ the exponent $\kappa(t)$ increases with increasing t reaching a value $\kappa_2 > 0$ and therefore $n(t)$ also starts to increase again for $t_a \ll t \ll t'_a$ reaching a new constant value $n_2(v)$ for $t \gg t'_a$. Matching with (4.71) and (4.72) yields

$$n(t) = n_Q + (vt_0)^{2\eta(1-\kappa_2)} \bar{n}'(t/t'_a) \quad (4.78)$$

and therefore $n_2(v) - n_Q \sim (vt_0)^{2\eta(1-\kappa_2)} \xrightarrow{v \rightarrow 0} 0$. For $\gamma > 2$ this second plateau of $n(t)$ is missing, the conclusions are, however, unchanged.

In order to give an estimate of the driving force one has to investigate the behavior of $\alpha(t)$, Eq.(2.20), first. In the plateau region $\alpha(t_p) \approx 0$ was found. Around $t \sim t_a$ it starts to increase and reaches a value $\alpha(t) \approx \gamma + 1$ for $t_a \ll t \ll t'_a$. Around $t \sim t'_a$ it starts to increase again reaching its asymptotic value $\alpha(t) = 2(\gamma + 1)$ for $t \gg t'_a$. The integral in the expression (2.16) for the driving force gets its main contribution from s such that $1 + \nu(s) - \alpha(s) = 0$. For $\gamma > 1$ this is fulfilled for $s \sim t_a$ and $n(t)$ is well approximated by n_Q . This yields the following relation between mean velocity and driving force:

$$F = (vt_0)^\eta \bar{F} \quad (4.79)$$

with

$$\bar{F} = -\frac{2\beta}{1+n_Q} \int_0^\infty dx x f''(\bar{q}(x)) \partial_x \bar{q}(x) \quad (4.80)$$

which does not depend on v . For given force the velocity increases slowly with increasing force according to

$$v \sim F^{1/\eta}. \quad (4.81)$$

This behavior is a form of creep.

In the one-dimensional case [2] creep has also been found for $\frac{1}{2} < \gamma < 1$ with

$$v \sim e^{aF^\mu} \quad (4.82)$$

with $\mu = 2(\gamma - 1)/(2\gamma - 1)$. A power law dependence of the above form (4.81) is obtained for $\gamma = 1$. Note that a

different definition of γ is used in [2]. The results quoted here refer to the present definition (2.5).

The parameter n_Q can be determined from the condition (4.4) which is equivalent to the requirement $D(t_p) = 0$. The main contribution to the integral comes from the region where $\nu(s) - \alpha(s) = 0$ which is again the case for $s \sim t_a$. With $n(s) \approx n_Q$ the result (4.24) is recovered and n_Q indeed agrees with the value derived within the QFDT-solution.

It is remarkable that the longest time scale in phase \mathcal{A} is not the external time scale v^{-1} but rather $t'_a \sim v^{-1-\eta}$, which is longer. The ultimate reason for that is the behavior of $\kappa(t) = \kappa_1 < 0$ at the border between the plateau and the asymptotic regime. This value also enters the exponent η , (4.74).

4.6.2 Phase \mathcal{B}

This is no longer the case in phase \mathcal{B} . The choice

$$t_a \sim v^{-1} \quad (4.83)$$

allows to rewrite the complete set of mean field equations for $t \sim t_a$ in terms of functions of t/t_a only, especially

$$n(t) = \bar{n}(t/t_a). \quad (4.84)$$

In the plateau region $n(t)$ is given by (4.59) and the dependence on c drops out for $c \ln(t/t_x) \sim \pi/2$, or with (4.64) for $t \sim e^{\pi/c} t_p$. Matching with (4.84) yields

$$t_a \sim e^{\pi/c} t_p. \quad (4.85)$$

On the other hand, (4.69) results from matching $q(t)$ and therefore

$$c = \frac{\pi}{(\zeta - 1) \ln(t_0 v)}. \quad (4.86)$$

This means $c = c(v) \rightarrow 0$ for $v \rightarrow 0$ as proposed earlier. With (4.64) the intermediate time scale t_x is

$$t_x \sim t_0^{(1-\zeta)/2} v^{-(1+\zeta)/2}. \quad (4.87)$$

The force necessary to sustain the velocity v has to be calculated from (2.16). The main contribution comes as before from the region where $1 + \nu(s) - \alpha(s) = 0$, which is the case for $s \sim t_a$. Using the scaling form $q(t) = \bar{q}(t/t_a)$, (3.5), and (4.84) yields

$$\begin{aligned} F &= F_p \\ &= -2\beta \int_0^\infty dx x f''(\bar{q}(x) + x^2) \frac{\partial_x \bar{q}(x)}{1 + \bar{n}(x)} \end{aligned} \quad (4.88)$$

This does not depend on v and therefore a finite pinning force F_p exists, which has to be overcome in order to set the particle in motion.

4.6.3 Phase \mathcal{C}

In phase \mathcal{C} again

$$t_a = v^{-1} \quad (4.89)$$

has to be chosen and matching to (4.66) requires $t_x = t_a$. Otherwise the same arguments as above (phase \mathcal{B}) hold and there is again a finite pinning force given by (4.88). The main difference between phase \mathcal{B} and \mathcal{C} is the value of $n(t)$ for $t_p \ll t \ll t_a$, which is finite in phase \mathcal{B} and essentially zero in phase \mathcal{C} .

It is again of interest to compare this result with the one-dimensional case [1, 2] where a finite pinning force is found for $\gamma = \frac{1}{2}$, whereas the pinning force diverges for $\gamma < \frac{1}{2}$. This divergence is due to the fact that no short distance cutoff in the correlation of the disorder is used in the one-dimensional calculation. This is also the reason why the phase boundaries in this case do not depend on temperature.

4.7 The phase diagram

Let me summarize the results regarding the phase diagram and the dependence of $v(F)$. Depending on temperature T and exponent γ several phases have been found. The above considerations yield the phase diagram shown in Fig.1 and discussed in more detail below. Different dependencies of the velocity on the driving force are observed in different phases. Examples are shown in Fig.15.

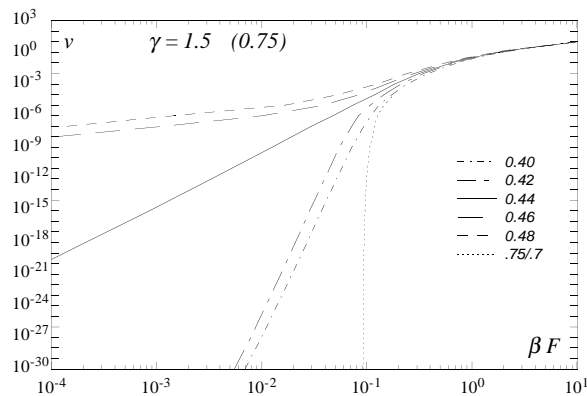


Figure 15: Drift velocity as a function of the applied force in phase \mathcal{O} , \mathcal{A} , \mathcal{B} and at the boundary between phase \mathcal{O} and \mathcal{A} .

The curve marked .75/.7 belongs to $\gamma = 0.75$ and $T = 0.7$, which is in phase \mathcal{B} . This point is also used for the examples presented in Section 3.2. Pinning is clearly observed. With increasing force $v(F)$ becomes linear in F indicating a finite mobility $m = v/F$. Its value is determined by the first term in (2.16), which means that the influence of the random potential vanishes for high velocities.

The curves marked 0.40 and 0.42 correspond to $\gamma = 1.5$ and $T = 0.4$ and $T = 0.42$, respectively. Both points are in phase \mathcal{A} . The temperature $T = 0.4$ is the second example in Section 3.2. A power law dependence of $v(F)$ is found in accordance with the analytic investigations (4.81). For $\gamma = 1.5$ and $T = 0.4$ one finds $\eta = 0.053$. With increasing force again the free mobility is found. The curve marked 0.44 is right at the transition line $\gamma = 1.5$, $T = T_c(1.5) = 0.4387$, and $\eta = 0.19$ is found. The remaining curves marked 0.46 and 0.48 are in the high temperature phase \mathcal{O} with $T = 0.46$ and $T = 0.48$, respectively. For $v \rightarrow 0$ a finite mobility is found, which is much smaller than the free value. It vanishes at the critical temperature T_c .

4.7.1 Drift phase \mathcal{O}

For $T > T_c(\gamma)$, (4.14), and $\gamma > 1$ a finite mobility $m = v/F$ is found for $v \rightarrow 0$. It is given by (4.16) and it vanishes at the boundaries of this phase. There are no long time scales.

4.7.2 Creep phase \mathcal{A}

This phase is characterized by $n_Q < n_x$ given in (4.24) and (4.56). Its boundary with phase \mathcal{O} is $T = T_c(\gamma)$ and the boundary to phase \mathcal{B} is determined by $n_Q = n_x$. This yields with (4.8), (4.24) and (4.56)

$$\frac{f'(q_c) f'''(q_c)}{f''^2(q_c)} = 2 \left(1 + \frac{1}{6} \tilde{D}_x\right). \quad (4.90)$$

Inserting (2.5) one finds that this phase boundary is determined by $\gamma = \gamma_c$, with

$$\gamma_c = \frac{1}{1 + \frac{1}{3} \tilde{D}_x} \approx 1.3044. \quad (4.91)$$

For $v \rightarrow 0$ one observes creep in the form $v \sim F^{1/\eta}$, (4.81), with $\eta \rightarrow 0$ for $\gamma \rightarrow \gamma_c$.

4.7.3 Pinning phase \mathcal{B} and \mathcal{C}

This phase exists for $\gamma < 1$ or $T < T_c$ and $\gamma < \gamma_c$. It has a finite pinning force which has to be overcome in order to set the particle in motion. Phase \mathcal{B} and \mathcal{C} are distinct only by their value of $n(t)$ for $t_p \ll t \ll t_a$. In phase \mathcal{C} one finds $n(t) \approx 0$ for $t \ll t_a$ which means that the FDT holds up to this value, whereas it starts to be violated already for $t \sim t_a$ in phase \mathcal{A} and \mathcal{B} .

5 Discussion

The first aspect of this investigation deals with the motion of a particle in a correlated random potential with power law decay of the correlations under the influence of an applied driving force. The phase diagram shows

a phase with finite mobility, a creep phase and pinning phases. Similar behavior is found in a one-dimensional model [1, 2] indicating that the transitions found are not an artifact of the mean field treatment, which becomes exact in the limit of infinite dimensionality. In the creep phase $v(F)$ obeys a power law. Such a behavior is also found in the one-dimensional case, but only at the boundary between the drift and the creep phase, which is otherwise ruled by a stretched exponential law. The pinning phase in the present case has a finite pinning force, which is also found in the one-dimensional case, but only at the boundary between creep and pinning phase. Otherwise the pinning force diverges in this calculation, which can be traced back to the absence of a short distance cutoff of the power law decay of the correlations.

The numerical results indicate the existence of several scaling regimes which are verified by analytic investigations of the asymptotic properties in the limit of small drift velocity. These regimes are, with increasing time, the FDT-regime describing a local equilibrium within one of the valleys of the energy landscape, an intermediate plateau regime where the correlation function $q(t)$ stays close to the EA-order parameter q_c and where the characteristic time scale $t_p(v) \sim v^\zeta$, and the asymptotic regime with characteristic time scale $t_a \sim v^{-1}$. In the creep phase \mathcal{A} this asymptotic regime is ruled by two time scales, $t_a \sim v^{-1+\eta}$ and $t'_a \sim v^{-1-\eta}$. The exponent η also determines the power law of $v(F)$.

The numerical calculations have been performed for a wide range of velocities including values as small as 10^{-30} and over times ranging from 10^{-4} to 10^{36} . This is necessary in order to deduce the full asymptotic behavior and even at these extreme values part of the structure is not yet fully developed.

The second aspect relates to glassy non-equilibrium dynamics of mean field models. The model investigated here has several advantages in this respect. It uses Langevin dynamics which is certainly easier to handle than for instance Glauber dynamics in Ising type models. Depending on γ , continuous as well as discontinuous ergodicity breaking transitions are found. With applied external force a stationary non-equilibrium state is reached where correlation and response functions depend only on time differences. The inverse velocity v^{-1} plays the role of an external long time scale.

The replica treatment of this model [4, 5] predicts transitions between a phase with continuous replica symmetry breaking for $\gamma < \gamma_c = 1$, a 1RSB-phase for $\gamma > 1$ and $T < T_{c,1RSB}$, and a replica symmetric phase for $\gamma > 1$ and $T > T_{c,1RSB}$. The present phase diagram differs in the sense that $T_c > T_{c,1RSB}$ and $\gamma_c > 1$. A difference in T_c has been observed before in models with discontinuous transitions [6, 13, 14, 15]. This was traced back to the fact that the states contributing most to the

static replica calculation are different from those relevant for dynamics and are not accessible within finite time in the thermodynamic limit. The same now appears to be true for continuous transitions as well.

There have been several proposals regarding the long time dynamics. For the SK-model Sompolinsky and Zippelius [8, 9] proposed a hierarchical or ultrametric organization of long time scales. This can be rephrased as the postulate [11] that correlation and response functions can be expressed as functions of $x(t) = 1 - \ln t / \ln \bar{t}$ where \bar{t} is some long external time scale. It has, however, been shown that this leads to inconsistencies [12]. In the present formulation this requirement means $\nu(t) = 0$ for times where the hierarchy exists. This is not observed.

The assumption of an ultrametric hierarchy of time scales leads to results which are identical to those obtained by Parisi's continuous replica symmetry breaking scheme [10]. One of the quantities to be compared is the probability of overlaps $P(q)$ which is the derivative $P(q) = |\partial_q x(q)|$ of a function $x(q)$ which in dynamics is given by

$$x(q(t)) = \frac{1}{1 + n(t)}. \quad (5.1)$$

Within this scheme only $x(q)$ is determined, whereas correlation and response functions are not unique for long times. This is in contrast to the present investigation where correlation and response functions are unique for all times.

The function $x(q)$ obtained from replica theory and from the present investigation are compared in Fig.16. The difference between the results shows again that different states are of relevance in dynamics and replica theory.

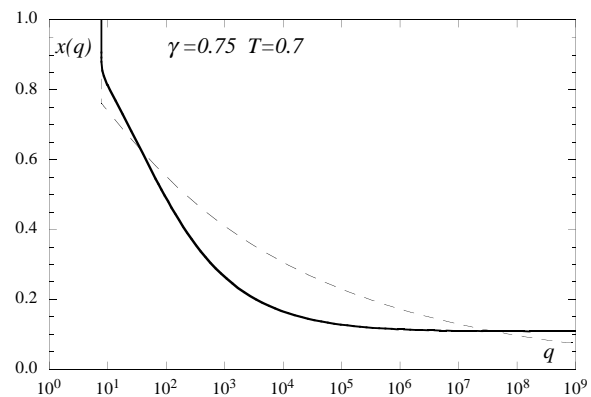


Figure 16: Function $x(q)$ in phase \mathcal{B} , see text. The results obtained in the present investigation (solid) and from replica theory (dashed) are shown.

For systems with discontinuous transitions [6, 13, 14, 15] the QFDT-solution has been proposed. It requires $n(t) \rightarrow n_Q$ for $t \sim \bar{t}$. This is actually found in phase \mathcal{A} . Within this scheme nothing can be said about the

generation of internal long time scales. Furthermore, the resulting correlation and response functions are again not uniquely determined, contrary to the present results.

There has been considerable interest on mean field dynamics of spin glasses and related systems with non-equilibrium initial conditions [20, 21, 22, 23, 24, 25, 26]. In the work of Cugliandolo and Dean [25] an exact solution of the spherical SK-model is reported. It shows aging phenomena although a replica calculation of this model does not require replica symmetry breaking. The remaining papers deal with models which have phases with broken replica symmetry (1-step or continuous). Various proposals are made for the long time properties of correlation and response functions depending on two time arguments t and t' . Again for $t - t' \rightarrow \infty$ and $t' \rightarrow \infty$ with finite $(t - t')/t'$ the resulting correlation and response functions could not be determined uniquely. This is likely to be due to an incomplete analysis of the plateau regime where $t - t' \sim t'^{\zeta}$ with $0 < \zeta < 1$.

A comparison with the present results certainly has to be taken with care because the specific non-equilibrium situation is different. Nevertheless using t' as external time scale one expects that at least the properties for times $t - t' \ll t'$ can be compared. This includes the plateau regime. A careful investigation of this regime and the kind of FDT-violation taking place there seems necessary in this case, too and this is likely to remove the arbitrariness in the correlation and response functions found so far.

A Dynamic mean field equations

Time dependent expectation values of products of the variables ϱ and $\hat{\varrho}$ can be represented as path integrals

$$\langle \mathcal{O}(\varrho, \hat{\varrho}) \rangle = \int \mathcal{D}\{\varrho, \hat{\varrho}\} \mathcal{O}(\varrho, \hat{\varrho}) \times \exp\left(-\sum_{\alpha} \{S_{\alpha}^o + S_{\alpha}^v\}\right) \quad (\text{A.1})$$

with

$$S_{\alpha}^o = \int dt \left\{ \hat{\varrho}_{\alpha}(t)^2 + i\hat{\varrho}_{\alpha}(t) \left[(\partial_t + \mu_0)\varrho_{\alpha}(t) + \sqrt{N}v\delta_{\alpha 1} - \beta F_{\alpha}(t) \right] \right\} \quad (\text{A.2})$$

and

$$S_{\alpha}^v = i\beta \int dt \hat{\varrho}_{\alpha}(t) \frac{\partial V(\varrho(t))}{\partial \varrho_{\alpha}(t)}. \quad (\text{A.3})$$

Averaging over the disorder with (2.4) results in

$$\sum_{\alpha} S_{\alpha}^v \rightarrow \bar{S}_v = -\frac{1}{2} \sum_{\alpha\beta} \overline{S_{\alpha}^v S_{\beta}^v} \quad (\text{A.4})$$

and the averaged action is

$$\begin{aligned} \bar{S}_v = \beta^2 \int dt dt' & \left\{ f'(x(t, t')) \sum_{\alpha} \hat{\varrho}_{\alpha}(t) \hat{\varrho}_{\alpha}(t') \right. \\ & + 2f''(x(t, t')) \frac{1}{N} \sum_{\alpha\beta} \hat{\varrho}_{\alpha}(t) \hat{\varrho}_{\beta}(t') \\ & \times \left[\varrho_{\alpha}(t) - \varrho_{\alpha}(t') + \sqrt{N}v(t - t')\delta_{\alpha 1} \right] \\ & \left. \times \left[\varrho_{\beta}(t) - \varrho_{\beta}(t') + \sqrt{N}v(t - t')\delta_{\beta 1} \right] \right\} \quad (\text{A.5}) \end{aligned}$$

with

$$\begin{aligned} x(t, t') = \frac{1}{N} \sum_{\alpha} & \left[\varrho_{\alpha}(t) - \varrho_{\alpha}(t') \right]^2 \\ & + \frac{2v(t - t')}{\sqrt{N}} \left[\varrho_1(t) - \varrho_1(t') \right] \\ & + v^2 [t - t']^2. \quad (\text{A.6}) \end{aligned}$$

This allows to calculate correlation functions (2.6), response functions (2.7), using

$$r(t - t') = \frac{1}{N} \sum_{\alpha} \langle \varrho(t) i\hat{\varrho}(t') \rangle, \quad (\text{A.7})$$

and other expectation values like $W(t)$, given by (2.4) and (2.11).

In mean field theory, see e.g. [6], an effective action is introduced replacing appropriate terms in the averaged action by their expectation values such that the whole problem separates. This effective action is in the present case

$$\begin{aligned} S_{\alpha}^{eff} = S_{\alpha}^o + \frac{1}{2} \int dt dt' & W(t - t') \hat{\varrho}_{\alpha}(t) \hat{\varrho}_{\alpha}(t') \\ & + i \int dt \int dt' w(t - t') r(t - t') \hat{\varrho}_{\alpha}(t) \\ & \times \left[\varrho_{\alpha}(t) - \varrho_{\alpha}(t') + \sqrt{N}v(t - t')\delta_{\alpha 1} \right]. \quad (\text{A.8}) \end{aligned}$$

The identity

$$\langle \mathcal{O}(\varrho, \hat{\varrho}) \frac{\delta S(\varrho, \hat{\varrho})}{\delta \hat{\varrho}(t)} \rangle = \langle \frac{\delta \mathcal{O}(\varrho, \hat{\varrho})}{\delta \hat{\varrho}(t)} \rangle \quad (\text{A.9})$$

can be used to derive the equations of motion and the driving force. The choice $\mathcal{O}(\varrho, \hat{\varrho}) = \hat{\varrho}(0)$ and the requirement of causality $r(t) = 0$ for $t \leq 0$ yields for $\alpha > 1$ the first mean field equation (2.8). With $\mathcal{O}(\varrho, \hat{\varrho}) = \varrho(0)$ for $\alpha > 1$ and (2.6) the second mean field equation (2.9) is found. The driving force (2.16) is obtained from $\mathcal{O}(\varrho, \hat{\varrho}) = 1$ for $\alpha = 1$.

Acknowledgement. I want to thank L. Cugliandolo, P.L. le Doussal, S. Franz, H. Kinzelbach, R. Kühn, J. Kurchan, M. Mézard and A. Zippelius for useful discussions. This work was partially supported by EC-contract CHRX-CT92-0063.

References

- [1] Sinai, Y. G.: Theor. Probab.Its Appl. **27**, 247 (1982).
- [2] le Doussal, P., Vinokur,V. M.: to be published (1995).
- [3] Scheidl, S.: Z.Physik B **97**, 345 (1995).
- [4] Mézard, M., Parisi, G.: J.Phys. A **23**, L1229 (1990).
- [5] Mézard, M., Parisi, G.: J.Phys. I France **1**, 809 (1991).
- [6] Kinzelbach, H., Horner, H.: J.Phys. I France **3**, 1329 (1993).
- [7] Kinzelbach, H., Horner, H.: J.Phys. I France **84**, 95 (1993).
- [8] Sompolinsky, H.: Phys. Rev. Lett **47**, 935 (1981).
- [9] Sompolinsky, H., Zippelius, A.: Phys. Rev. B **25**, 6860 (1982).
- [10] Parisi, G.: Phys. Rev. Lett. **43**, 1754 (1979).
- [11] Horner, H.: Z.Physik B **57**, 29 (1984).
- [12] Horner, H.: Z.Physik B **66**, 175 (1987).
- [13] Kirkpatrick, T.R., Thirumalai., D.: Phs. Rev. B **36**, 5388 (1987).
- [14] Horner,H.: Z.Physik B **86**, 291 (1992).
- [15] Crisanti, A., Horner, H., Sommers, H.-J.: Z.Physik B **92**, 257 (1993).
- [16] Kinzelbach, H., Horner, H.: Z.Phys B **3**, 1329 (1991).
- [17] Lundgren, L., Svedlindh, P., Nordblad, P., Beckman, O.: Phys. Rev. Lett. **51**, 911 (1983).
- [18] Chamberlin, R.V., Mozurkevich, G., Orbach, R.: Phys. Rev. Lett. **52**, 867 (1986).
- [19] Lefloch, F., Hamman, J., Ocio, M., Vincent, E.: Europhys. Lett **18**, 647 (1992).
- [20] Cugliandolo, L.F., Kurchan, J.: Phys. Rev. Lett. **71**, 173 (1993).
- [21] Franz, S., Mézard, M.: Europhys. Lett. **26**, 209 (1994).
- [22] Franz, S., Mézard, M.: Physica A **209**, 1 (1994).
- [23] Cugliandolo, L.F., Kurchan, J.: J.Phys A, **27**, 5749 (1994).
- [24] Baldassarri, A., Cugliandolo, L.F., Kurchan, J., Parisi, G.: J.Phys A, **28**, 1831 (1995).
- [25] Cugliandolo, L.F., Dean, D.S.: J.Phys A, to be published (1995).
- [26] Cugliandolo, L.F., le Doussal, P.: to be published (1995).